*Published online 31 October 2013* *Nucleic Acids Research, 2014, Vol. 42, No. 3* **2075–2084**
*doi:10.1093/nar/gkt1039*

# A cyclobutane thymine–$N^4$-methylcytosine dimer is resistant to hydrolysis but strongly blocks DNA synthesis

**Junpei Yamamoto[1], Tomoko Oyama[1], Tomohiro Kunishi[1], Chikahide Masutani[2], Fumio Hanaoka[3] and Shigenori Iwai[1,*]**

[1]Division of Chemistry, Graduate School of Engineering Science, Osaka University, 1-3 Machikaneyama, Toyonaka, Osaka 560-8531, Japan, [2]Research Institute of Environmental Medicine, Nagoya University, Furo-cho, Chikusa-ku, Nagoya 464-8601, Japan and [3]Faculty of Science, Gakushuin University, 1-5-1 Mejiro, Toshima-ku, Tokyo 171-8588, Japan

Received August 28, 2013; Revised October 9, 2013; Accepted October 10, 2013

## ABSTRACT

**Exposure of DNA to ultraviolet light produces harmful crosslinks between adjacent pyrimidine bases, to form cyclobutane pyrimidine dimers (CPDs) and pyrimidine(6–4)pyrimidone photoproducts. The CPD is frequently formed, and its repair mechanisms have been exclusively studied by using a CPD formed at a TT site. On the other hand, biochemical analyses using CPDs formed within cytosine-containing sequence contexts are practically difficult, because saturated cytosine easily undergoes hydrolytic deamination. Here, we found that *N*-alkylation of the exocyclic amino group of 2′-deoxycytidine prevents hydrolysis in CPD formation, and an *N*-methylated cytosine-containing CPD was stable enough to be derivatized into its phosphoramidite building block and incorporated into oligonucleotides. Kinetic studies of the CPD-containing oligonucleotide indicated that its lifetime under physiological conditions is relatively long (~7 days). In biochemical analyses using human DNA polymerase η, incorporation of TMP opposite the *N*-methylcytosine moiety of the CPD was clearly detected, in addition to dGMP incorporation, and the incorrect TMP incorporation blocked DNA synthesis. The thermodynamic parameters confirmed the formation of this unusual base pair.**

## INTRODUCTION

Ultraviolet (UV) light causes harmful effects in DNA, such as the formation of UV-induced damage, i.e. cyclobutane pyrimidine dimers (CPDs) and pyrimidine(6–4)pyrimidone photoproducts. The loss of genetic integrity caused by alterations in the chemical structure of DNA leads to carcinogenesis and mutagenesis (1). To protect their genetic information, organisms have developed UV protection systems. One of these systems is nucleotide excision repair (NER), in which several enzymes function together to remove the UV lesions. The lack of NER activity causes the inherent genetic disease, xeroderma pigmentosum (XP), which has been classified into seven complementation groups and a variant (XPA–G and XPV) (2). Among them, the protein encoded by *XPV* is not directly involved in the NER pathway, but is responsible for translesion DNA synthesis (TLS), in which special DNA polymerases, the Y-family polymerases, bypass the lesions during DNA synthesis instead of the replicative polymerases stalled at the damaged site (3). Human DNA polymerase η (hPolη), which is the *XPV* product (4), and its yeast ortholog, RAD30 (5), are involved in the error-free bypass of the *cis-syn* CPD formed at the TT site (T[]T), and incorporate two adenylates (6). A decade has passed since these enzymes were found, and now the molecular mechanisms of TLS are being elucidated (7,8).

The UV-induced DNA lesions are formed at bipyrimidine sites in DNA. Among the pyrimidine bases, cytosine plays an important role for functional development of organisms by undergoing epigenetic modification (9). Although cytosine is widely used for gene regulation, it is the most labile base and undergoes deamination to irreversibly form uracil, with a reaction rate constant of $1 \times 10^{-10}\,s^{-1}$ under physiological conditions (10). Upon CPD formation, hydrolytic deamination becomes accelerated to $3.9 \times 10^{-5}\,s^{-1}$ (11). The uracil-containing CPD is easily formed, and can cause the C→T transition

*To whom correspondence should be addressed. Tel: +81 6 6850 6250; Fax: +81 6 6850 6240; Email: iwai@chem.es.osaka-u.ac.jp

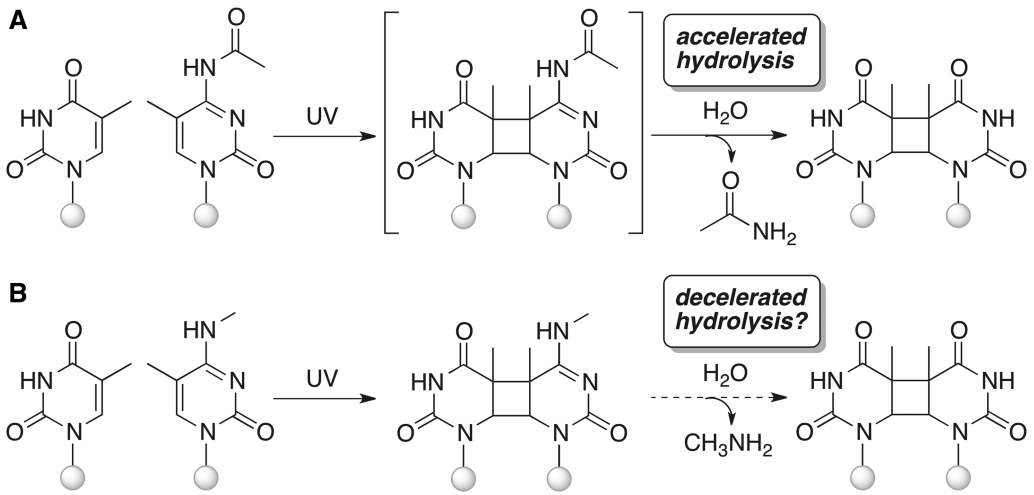


**Figure 1.** Formation of cyclobutane thymine–cytosine dimers modified with **(A)** acetyl or **(B)** methyl groups at the exocyclic amino function. In our previous work (A), the acetyl group clearly accelerated hydrolysis after CPD formation.

mutation (12,13). On the other hand, 5-methylcytosine (mC) is more stable to hydrolysis than unmodified cytosine (14,15). Taylor and coworkers addressed the problem of the lability of the cytosine-containing CPD by using mC, instead of intact cytosine. They successfully prepared and purified short oligonucleotides containing the mC-CPD, and analyzed TLS by yeast and human DNA polymerase η (16,17).

Taking into account the fact that the methylation at the C5 position of cytosine stabilizes the C–N bond, methylation at the N4 position of cytosine would also reduce the frequency of hydrolysis, due to the electron-donating ability of the methyl group. We recently reported that the modification of the exocyclic amino group with an electron-withdrawing acetyl group drastically facilitated the hydrolytic removal of the acetylamino group, even in the presence of the methyl group at the C5 position (Figure 1) (18). A thymine-containing CPD was formed, in this case. Since the modification of this amino group can directly modulate the electron density of the C4 position, where the nucleophilic attack of a water molecule occurs, the attachment of an electron-donating methyl group to the amino group was expected to reduce the deamination rate. In fact, the stability of $N^4$-methylcytosine to hydrolysis was suggested in several literatures (19,20), but no obvious evidence has been reported thus far.

Here, we report that the photosensitized cycloaddition of partially protected thymidylyl-(3′→5′)-2′-deoxy-$N^4$,5-dimethylcytidine (compound **4** in Scheme 1) afforded a stable CPD, without the loss of the methylamino group in the cytosine moiety. Furthermore, the obtained CPD, formed between thymine and $N^4$,5-dimethylcytosine (T[]$mC^m$), was quite stable under various synthetic conditions, and thus we successfully synthesized its phosphoramidite building block and oligonucleotides containing the *cis-syn* T[]$mC^m$ on a DNA synthesizer. These oligonucleotides were utilized to investigate the thermodynamic and biochemical properties of the cyclobutane thymine–$N^4$-methylcytosine dimer.

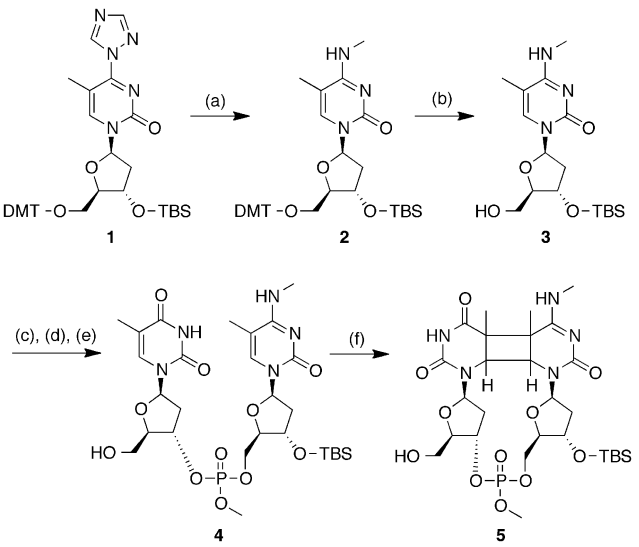


**Scheme 1.** Synthesis of the CPD, formed between thymidine and 2′-deoxy-$N^4$,5-dimethylcytidine. Reagents and conditions: (a) methylamine/acetonitrile, water, (b) 80% acetic acid, (c) 5′-*O*-DMT-thymidine-3′-methyl-*N*,*N*-diisopropylphosphoramidite, tetrazole/acetonitrile, (d) $I_2$, $H_2O$/THF (e) 80% acetic acid and (f) UV (>280 nm), acetophenone/$H_2O$, acetonitrile.

## MATERIALS AND METHODS

### General

Reagents for DNA synthesis were purchased from Applied Biosystems Japan (Tokyo, Japan) and Glen Research (Sterling, VA, USA). All other reagents and solvents were purchased from Wako Pure Chemical Industries, Ltd. (Osaka, Japan) or Sigma-Aldrich (St. Louis, MO, USA). TLC analyses were performed on Merck Silica gel 60 F254 plates, and the results were visualized by UV illumination at 254 nm. For column chromatography, Wakogel C-200 and C-300 were used for practical and precise separations, respectively. HPLC

analyses were performed on a Shimadzu gradient-type analytical system equipped with a Shimadzu SPD-M10AVP photodiode-array detector. A Waters μBondasphere C18 5 μm 300 Å column (3.9 mm × 150 mm) was used on this system, at a flow rate of 1.0 ml $min^{-1}$, with a linear gradient of acetonitrile in 0.1 M triethylammonium acetate (TEAA) (pH 7.0) generated over 20 min. $^{1}H$ and $^{31}P$ NMR spectra were measured on a Varian INOVA 500 spectrometer. $^{1}H$ chemical shifts were calibrated with tetramethylsilane (TMS) in the deuterated solvents. In the $D_2O$ solution, the chemical shifts were indirectly calibrated with sodium 4,4-dimethyl-4-silapentane-1-sulfonate, as an external reference. $^{31}P$ chemical shifts were calibrated with trimethylphosphate, as an external reference. Two-dimensional phase-sensitive NOESY and ROESY spectra were acquired with mixing times of 700 and 350 ms, respectively. High-resolution mass spectrometry was performed on a JEOL JMS-700 spectrometer with fast atom bombardment ionization.

### Formation of the *cis-syn* cyclobutane thymine–$N^4$, 5-dimethylcytosine dimer, T[]mC$^m$

A 1 mM solution of compound **4** dissolved in 50% aqueous acetonitrile (1.3 l) was prepared, and the solution was purged with nitrogen for 5 min. After the addition of acetophenone (1.22 ml, 10.4 mmol), the solution was irradiated in a Pyrex immersion well apparatus fitted with a 450-W high-pressure mercury lamp (UM-452; Ushio, Tokyo, Japan) in a 4°C water bath. Aliquots (200 μl) of the reaction mixture were sampled at appropriate intervals and were evaporated to dryness. The residues were dissolved in water (200 μl), and the samples were immediately analyzed by HPLC, using a 27.5–36.5% acetonitrile gradient generated over 20 min. After 2 h, the solution was concentrated to dryness. To determine the product structures, the crude products were roughly separated on a Preparative C18 125 Å column (Waters Corporation, Milford, MA, USA) installed on a BioLogic LP chromatographic system (Bio-Rad Laboratories, Hercules, CA, USA). An acetonitrile gradient of 25–37.5% was generated over 400 min. Finally, the reaction was repeated six times, using 5.69 g of compound **4** (8.28 mmol) in total. The collected residues were purified by column chromatography using Wakogel C-300 with a stepwise gradient of 0–10% methanol in $CHCl_3$. The pooled fractions were concentrated to dryness to give the *cis-syn* isomer of compound **5**. Yield 420 mg (611 μmol, 7.3%).

### Oligonucleotide synthesis

The phosphoramidite building blocks of the *cis-syn* TT-CPD (T[]T) and 4-triazolothymidine were synthesized according to the previous reports (21,22). These building blocks and compound **8** (described in Supplementary Data) were dissolved in anhydrous acetonitrile at a concentration of 0.13 M and were installed on an Applied Biosystems 3400 DNA synthesizer. Solutions of nucleoside phosphoramidites for ultramild DNA synthesis (Glen Research), as well as the base-unprotected thymidine phosphoramidite, were also installed. Phenoxyacetic anhydride and 1-methylimidazole were used as the capping reagents (23). Two types of 12-mers, d(CGTACT[]mC$^m$CATGC) (T[]mC$^m$ 12-mer) and d(CAT[]mC$^m$AGCACGAC), and a 30-mer, d(CTCGTCAGCATCT[]mC$^m$CATCATACAGTCAGTG) (T[]mC$^m$ 30-mer), were synthesized on the 1 μmol scale, by using the standard synthetic program modified only in the reaction time for the coupling of the *cis-syn* T[]mC$^m$ building block (20 min). After the synthesis, the supports were treated with a thiophenol solution (thiophenol/TEA/THF = 1/2/2, v/v/v) for 1 h, successively washed with THF (1 ml × 1), methanol (2 ml × 5) and then acetonitrile (2 ml × 3), and treated with 28% ammonia water (2 ml) at room temperature for 2 h. The obtained oligonucleotides were analyzed and purified by HPLC with linear gradients of 5–13% and 7–13% acetonitrile for the 12-mers and 30-mer, respectively. The column was run at ambient temperature, to prevent the hydrolysis of T[]mC$^m$ during the purification. The pooled solution was evaporated to dryness, and the residue was dissolved in water (500 μl). The solution was passed through an illustra$^{TM}$ NAP-5 column (GE Healthcare, Buckinghamshire, UK) to remove TEAA. The T[]mC$^m$ 12-mer was characterized by LC-ESI mass spectrometry (Supplementary Figure S1), and its molecular mass was determined as $m/z$ 3608.66, which is identical to the calculated value ($[M–H]^-$, 3608.40). The two 12-mers containing T[]T, d(CGTACT[]TCATGC) (T[]T 12-mer) and d(CAT[]TAGCACGAC), were synthesized using the *cis-syn* TT-CPD phosphoramidite. A 12-mer oligonucleotide containing $N^4$,5-dimethylcytosine, d(CATmC$^m$AGCACGAC), was prepared by using the 4-triazolothymidine phosphoramidite.

### Temperature dependence of the hydrolysis reaction in the T[]mC$^m$ 12-mer

Solutions (1 ml) of the T[]mC$^m$ 12-mer (20 nmol), in 180 mM phosphate buffer (pH 7.4), were placed in plastic tubes and incubated at 50, 80 and 95°C. At appropriate intervals, aliquots (50 μl) of the reaction mixture were immediately analyzed by HPLC. Fractions of the starting product were plotted on a logarithmic vertical axis against the incubation time. The Arrhenius plot was produced using $k_{obs}$.

### Translesion synthesis across the *cis-syn* T[]mC$^m$ by human DNA polymerase η (hPolη)

The 5′-$^{32}$P-labeled primer-template was prepared by mixing either the 16-mer primer d(CACTGACTGTATGATG), the G-ended 17-mer primer (dG17) d(CACTGACTGTATGATGG) or the T-ended 17-mer primer (T17) d(CACTGACTGTATGATGT), labeled at their 5′ ends, with each of the 30-mer templates, d(CTCGTCAGCATC$\overline{XY}$CATCATACAGTCAGTG), where the underlined $\overline{XY}$ represents the lesion site, at a molar ratio of 1:1. Standard reaction mixtures (10 μl), containing 40 mM Tris–HCl (pH 8.0), 1 mM $MgCl_2$, 100 μM dNTPs, 10 mM DTT, 0.24 mg $ml^{-1}$ BSA, 60 mM KCl, 2.5% glycerol, 40 nM 5′-$^{32}$P-labeled primer-template and His-tagged human DNA polymerase η (4,6), were

incubated at 37°C. Mixtures (10 µl) for the reaction of exonuclease-deficient Klenow fragment (KF), containing 10 mM Tris–HCl (pH 7.9), 50 mM NaCl, 10 mM $MgCl_2$, 1 mM dithiothreitol, 40 nM the labeled primer-template and KF, were incubated at 37°C as well. The reactions were terminated by the addition of stop solution (10 µl), containing 95% formamide, 20 mM EDTA, 0.025% bromophenol blue and 0.025% xylene cyanol. These mixtures were heated at 95°C for 10 min, and then the reaction products were separated by electrophoresis on a 20% polyacrylamide/7.5 M urea gel. The dried gels were analyzed with a GE Healthcare FLA7000 image analyzer.

The kinetic analysis was performed under single-completed hit conditions (24), essentially according to the previous report (25). The standard reaction mixtures (10 µl), containing six different concentrations of dNTPs, were incubated at 37°C for three different incubation times, and the reactions were terminated by the addition of stop solution (10 µl). The reaction products were analyzed by electrophoresis as mentioned above, and the amounts of the extended products on the dried gels were quantified with the Multi Gauge software, version 3.1 (Fuji Film). In the experiment, the concentrations and the incubation times were appropriately set, so the amounts of the extended products would not exceed 20% of the total density. The determination of the velocities at each concentration of dNTPs was performed three times, and the averaged velocities were plotted against the concentrations. To obtain the Michaelis parameters, the plot was fitted with the Michaelis–Menten equation, $v = V_{max}$ [S]/($K_m$ + [S]), by the non-linear least squares approach, calculated with the Origin 7.0 software. The catalytic rate constants ($k_{cat}$) were obtained by the equation $k_{cat}$ = [$V_{max}$ (mol of the primer-template)/(mol of DNA polymerase)].

### Thermodynamic analysis of the formation of duplexes mimicking the primer-template structures

Lesion-containing 12-mers, d(CAXYAGCACGAC), where the underlined XY represents either TT, T[]T, TC, $TmC^m$ or T[]$mC^m$, were hybridized to dN-ended 9-mers, d(GTCGTGCTN) (4 nmol each), in a buffer containing 10 mM phosphate, 100 mM NaCl and 0.1 mM EDTA, pH 7.0 (50 µl), by heating at 65°C for 5 min and cooling to room temperature overnight. Under the annealing conditions, ~5% of T[]$mC^m$ was hydrolyzed to T[]T. Each of the duplex solutions was diluted with the same buffer to total concentrations ($C_t$) of 4.27, 5.97, 8.53, 11.95 and 17.1 µM. Melting curves were measured at 260 nm on a Shimadzu PharmaSpec UV-1700 UV/Vis spectrophotometer equipped with a TMSPC-8 temperature controller module. The temperature was raised from 18 to 70°C at a rate of 0.5°C $min^{-1}$, and the $T_m$ values were obtained by the two-point average method, using the data processing software supplied by the manufacturer. The measurements were repeated three times, and the averaged $T_m$ values were used for the following analyses.

To obtain the thermodynamic parameters, a van't Hoff analysis was performed, according to the previous report (26). The reported equation $1/T_m = R/\Delta H^\circ \ln(C_t/4) + \Delta S^\circ/\Delta H^\circ$ was employed for the fitting of the van't Hoff plot, on the basis of the bimolecular association of two non-self-complementary strands (27), and the $1/T_m$ values obtained for each $C_t$ were plotted over ln ($C_t$/4). The slope ($m$) and the $y$-intercept ($b$) of the linear least-square fitting correspond to $R/\Delta H^\circ$ and $\Delta S^\circ/\Delta H^\circ$, respectively. The Gibbs free energies of the association of the two strands at 25°C ($\Delta G^\circ$) were obtained by substituting $\Delta H^\circ$ and $\Delta S^\circ$ into the equation $\Delta G^\circ = \Delta H^\circ - T\Delta S^\circ$. The error analysis was then performed, and the variances and the covariance of the linear fitting ($\sigma_m^2$, $\sigma_b^2$ and $\sigma_{bm}$, respectively) were first obtained, according to the literature (28). The variances of $\Delta H^\circ$, $\Delta S^\circ$ and $\Delta G^\circ$ were calculated using the previously reported equation (29), and then the standard deviations were obtained by calculating the square roots of the variances.

## RESULTS

### Synthesis of oligonucleotides containing the *cis-syn* cyclobutane thymine–$N^4$,5-dimethylcytosine dimer, T[]$mC^m$

The thymidylyl-(3′→5′)-2′-deoxy-$N^4$,5-dimethylcytidine derivative **4**, in which the exocyclic amino group of cytosine was methylated, was synthesized from a 4-triazolothymidine derivative (Scheme 1), and photosensitized [2 + 2] cycloaddition of compound **4** was performed, according to the previous report (18). We first tested a different compound possessing a 2-cyanoethyl group in the internucleoside phosphotriester, as the starting material for this reaction. However, the HPLC analysis revealed that the starting material was significantly degraded during the UV irradiation (data not shown), probably due to the loss of the labile 2-cyanoethyl group upon the irradiation. To improve the stability in the photoreaction, the 2-cyanoethyl group was replaced by a methyl group (30).

The irradiation of compound **4** with a high-pressure mercury lamp in the presence of photosensitizer mainly yielded four peaks in the HPLC analysis after 2 h, and these products were referred to as peaks i–iv, in order of elution (Figure 2). The loss of the original absorption band of compound **4** in the UV absorption spectra of these products suggested that these products were cycloadducts (compound **5**). To identify their stereochemistry, they were roughly purified by reversed-phase column chromatography. Although these four peaks were not separated well on the reversed-phase column, we successfully isolated the product that yielded peak i. The ROESY spectrum of the purified product revealed that the characteristic correlations of H1′–H6 and H2′–H6 in the 5′ and 3′ components, respectively, as observed in our previous study (Supplementary Figure S2) (18). This result showed that the configuration of the cyclobutane ring between the two bases was *trans-syn*, with the SYN-ANTI conformation of the *N*-glycosidic bonds. Its exact mass was determined as $m/z$ 688.2770 ($[M+H]^+$; calcd for $C_{28}H_{47}N_5O_{11}PSi$, 688.2779), which demonstrated that the methylamino group of the *trans-syn* (SYN-ANTI) cycloadduct was intact. The products that yielded peaks

i and ii were treated with TEA•3HF and thiophenol in turn, to remove the protecting groups. We found that the deprotection of the products (peaks i and ii) gave the same product (data not shown), indicating that peak ii was the other *trans-syn* (SYN-ANTI) diastereomer caused by the chiral phosphotriester group. The products yielding peaks iii and iv were treated with TEA•3HF and thiophenol in the same manner, and their deprotection products were found to be identical to each other, but not to that obtained from the compounds yielding peaks i and ii (data not shown). After HPLC purification of this deprotection product (referred to as compound **9**), its NMR and mass spectra were measured. In the NOESY spectrum of compound **9** measured in $D_2O$, correlations of H2′–H6 in both the 5′ and 3′ components were observed (Supplementary Figure S3), indicating that its stereochemistry was *cis-syn* with the ANTI-ANTI conformation. Since the mass analysis of compound **9** also supported the presence of the methylamino group, peaks iii and iv were the $S_p$ and $R_p$ diastereomers of the *cis-syn* (ANTI-ANTI) structure of compound **5**. Fortunately, one of the *cis-syn* diastereomers (peak iv) was purified by silica-gel column chromatography, in the best isolated yield of 7.3%, and was characterized by NMR spectroscopy and mass spectrometry. Since the yield was not high, we repeated the 2 h irradiation of compound **4** six times, to compensate for the low yield, and finally the *cis-syn* isomer of compound **5** was obtained in an amount sufficient for the oligonucleotide synthesis.

Next, the chemical stability and reactivity of the methylamino group within the obtained CPD (T[]mC$^m$) were verified, to prepare its phosphoramidite building block. The dinucleoside monophosphate of the *cis-syn* T[]mC$^m$ (**9**) was quite stable to treatments with 80% $CH_3COOH$ for 1 h or 28% ammonia water for 2 h at ambient temperature (Supplementary Figure S4), which simulated the detritylation and ultra-mild deprotection conditions in the oligonucleotide synthesis, respectively. To test the reactivity with the capping reagents in the oligonucleotide synthesis, we used the abundant diastereomer of *trans-syn* (SYN-ANTI) T[]mC$^m$ (**5**), to save the *cis-syn* isomer. The isolated *trans-syn* isomer of compound **5** (peak i in Figure 2) was treated with excess amounts of phenoxyacetic anhydride in the presence of 1-methylimidazole, to determine whether the methylamino group could be acylated with the capping reagents. Considering the steric hindrance at the reactive amidine groups in the stereoisomers of compound **5**, the *cis-syn* T[]mC$^m$ was expected to be inert to the reaction if the *trans-syn* T[]mC$^m$, which contains less hindered amidine, was not acylated. After 2 h, the product was purified by silica-gel column chromatography and was treated with 28% ammonia water for 2 h. After these treatments, the intact *trans-syn* T[]mC$^m$ (**5**) was retained, indicating that the methylamino group of the *trans-syn* T[]mC$^m$ did not react with the capping reagents. These comprehensive results suggested that T[]mC$^m$ is chemically stable to the reactions in the oligonucleotide synthesis. After 5′-protection, 3′-deprotection and 3′-phosphitylation, the building block of the *cis-syn* T[]mC$^m$ (**8**) was successfully synthesized (Scheme 2).

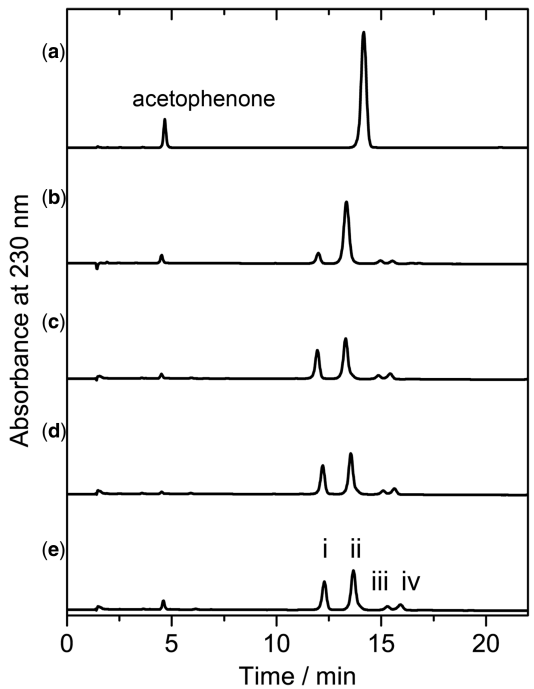


**Figure 2.** HPLC analysis of the cycloaddition reaction of *N*-methylated dinucleoside monophosphate (**4**) in the presence of photosensitizer, monitored at 230 nm. Aliquots of the reaction mixture were analyzed after UV irradiation for 0 (a), 0.5 (b), 1 (c), 1.5 (d) and 2 h (e).

## Synthesis and characterization of the oligonucleotides containing T[]mC$^m$

A 12-mer oligonucleotide containing the *cis-syn* T[]mC$^m$, d(CGTACT[]mC$^m$CATGC), was synthesized on a DNA synthesizer, and was purified by HPLC. The ESI-LC mass spectrometry revealed that the molecular weight of the

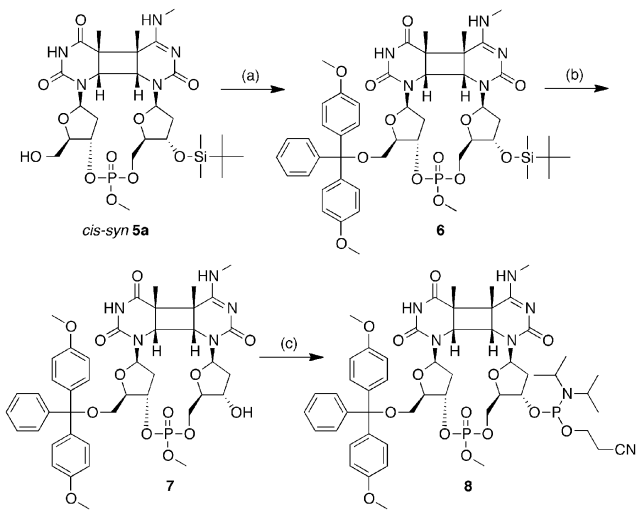


**Scheme 2.** Synthesis of the phosphoramidite building block of the *cis-syn* isomer of T[]mC$^m$. Reagents and conditions: (a) DMTCl/pyridine, (b) TEA•3HF/THF and (c) 2-cyanoethyl *N*,*N*-diisopropylchlorophosphoramidite, ethyldiisopropylamine/THF.

purified oligonucleotide was identical to the calculated value, demonstrating the presence of the methylamino group (Supplementary Figure S1). This result also supported that the *cis-syn* T[]mC$^m$ was inert to the capping reaction. The oligonucleotide was characterized further by UV irradiation and an enzymatic reaction. Both the UV irradiation of the T[]mC$^m$ 12-mer and the treatment with *Escherichia coli* CPD photolyase yielded a single product, which co-eluted with the TmC$^m$ 12-mer (Supplementary Figure S5). Although the desired product was obtained, we detected an extra peak, in addition to that of the desired product, in the HPLC analysis after the purification of the T[]mC$^m$ 12-mer (Supplementary Figure S5, trace a). The newly emerged minor peak co-eluted with an oligonucleotide containing the *cis-syn* TT-CPD (T[]T), suggesting that hydrolysis occurred at the methylamino group. We found that the hydrolysis was caused by the repeated coevaporations with water to remove TEAA after the HPLC purification.

Since the hydrolyzed product was detected in the HPLC analysis, the thermal stability of the methylamino group within T[]mC$^m$ to hydrolysis was investigated in detail. A solution of the T[]mC$^m$ 12-mer, dissolved in phosphate buffer at pH 7.4, was incubated at 50, 80 and 95°C, and aliquots were analyzed by HPLC at appropriate intervals. Upon the incubation, the T[]mC$^m$ 12-mer was converted into the T[]T 12-mer. The logarithm of the decreasing fraction of T[]mC$^m$ 12-mer was plotted against the incubation time, and these data were fitted with a pseudo-first order equation to obtain the observed rate constants ($k_{obs}$) (Supplementary Figure S6A). From $k_{obs}$, the half-lives ($\tau_{1/2}$) were calculated, as shown in Table 1. The $\tau_{1/2}$ of T[]mC$^m$ at 50°C was found to be 51 h, and extrapolation of our results indicated that its half-life under physiological conditions (37°C at pH 7.4) was 176 h, i.e. >7 days. From the Arrhenius plot of the obtained $k_{obs}$ (Supplementary Figure S6B), the activation energy of hydrolysis ($E_a$) and the frequency factor ($A$) were determined as 77.7 kJ mol$^{-1}$ and $7.97 \times 10^8$ min$^{-1}$, respectively.

### Translesion synthesis past T[]mC$^m$ by human DNA polymerase η (hPolη)

A longer oligonucleotide, T[]mC$^m$ 30-mer, was synthesized to investigate the biochemical properties of T[]mC$^m$, and primer extension analysis was performed using KF, which is deficient in the exonuclease activity, and human DNA polymerase η (hPolη). While KF extended the $^{32}$P-labeled 16-nucleotide (nt) primer hybridized to the TT template, no extended products were observed for the templates containing the *cis-syn* T[]T and *cis-syn* T[]mC$^m$ (Figure 3B, lanes 1–5 and 10–12), indicating that T[]mC$^m$ blocks chain elongation by replicative polymerases, as demonstrated for T[]T. hPolη, which is responsible for the error-free bypass of T[]T (lanes 6–8 in Figure 3B), successfully bypassed T[]mC$^m$ and extended the primer to the 30-mer, although the polymerase was considerably stalled at the site opposite the 3′ component of T[]mC$^m$ (lanes 13–15).

To determine which nucleotides are incorporated opposite T[]mC$^m$, the primer extension analysis was performed in the presence of each dNTP. hPolη mainly incorporated dGMP and TMP opposite the mC$^m$ moiety of T[]mC$^m$, as the 17th nucleotide of the primer (Figure 3C). To investigate which nucleotide was preferentially incorporated, kinetic analysis of the incorporation was performed under single-completed hit conditions. The initial velocities of the reactions were well-fitted with the Michaelis–Menten equation (Supplementary Figure S7), and the catalytic rate constants ($k_{cat}$) and the Michaelis constants ($K_m$) were obtained by non-linear least squares regression (Table 2). A comparison of the efficiencies, namely $k_{cat}/K_m$, clearly showed that the incorporation of TMP was unexpectedly efficient, and just 1.7-fold less frequent than that of dGMP. These results suggested that hPolη slightly preferred to incorporate dGMP as the correct nucleotide opposite the mC$^m$ moiety of T[]mC$^m$, but also incorporated the incorrect TMP at a relatively high efficiency.

Since the misincorporation of TMP at the 17th position of the primer could block further extension of the primer, the analysis using 17-nt templates containing dGMP or TMP at the 3′ end (dG17 or T17, respectively) was performed. As expected, almost no extended product was observed for T17, whereas hPolη extended the dG17 primer and incorporated dAMP opposite the 5′ component of T[]mC$^m$ (Figure 3D). These results indicated that TLS across T[]mC$^m$ could occur in an error-free manner once hPolη incorporated dGMP opposite the mC$^m$ of T[]mC$^m$, but more than 30% of the primer extension stopped at the site opposite the mC$^m$ moiety, due to the misincorporation of TMP.

**Table 1.** Half-lives ($\tau_{1/2}$) and Arrhenius parameters of T[]mC$^m$ and T[]mC hydrolysis in the oligonucleotides

| | Half-lives ($\tau_{1/2}$) (h) | | | Arrhenius parameters | |
|---|---|---|---|---|---|
| | 37°C | 50°C | 80°C | $E_a$ (kJ mol$^{-1}$) | $A$ (min$^{-1}$) |
| T[]mC$^m$ [a] | 176 [b] | 51.3 | 4.8 | 77.7 | $7.97 \times 10^8$ |
| T[]mC | 8.25 [c] | 2.13 [c] | 0.14 [b] | 86.5 | $5.16 \times 10^{11}$ |

[a]This work.
[b]These values were estimated by extrapolation with the Arrhenius plot in Supplementary Figure S6.
[c]Half-lives for T[]mC at 37 and 50°C were extracted from (17).

### Thermodynamic analysis of the formation of duplexes mimicking the primer-template structures

To investigate the mispairing ability of the mC$^m$ moiety of T[]mC$^m$ with TMP, a thermodynamic analysis was performed using short oligonucleotides mimicking the primer-template structure. The 12-mer oligonucleotides, d(CAXYAGCACGAC), where XY represents TT, TC, TmC$^m$, T[]T or T[]mC$^m$, were hybridized to the dN-ended 9-mer oligonucleotides, d(GTCGTGCTN), and the thermodynamic parameters for the duplex formation were obtained by the van't Hoff plot of the melting temperatures (Supplementary Figure S8; Table 3). In this system, the 12-mers and 9-mers mimic the templates and primers, respectively, and therefore, the differences between the obtained parameters could be used to

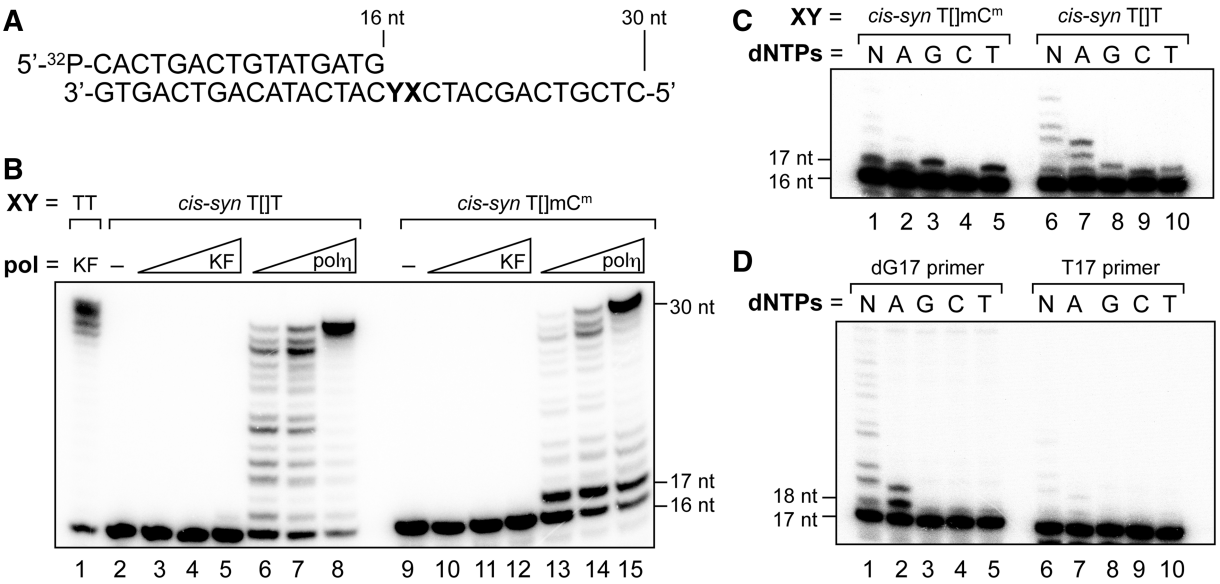


**Figure 3.** **(A)** Structure of the $^{32}$P-labeled 16-mer primer and the 30-mer templates for TLS by hPolη. XY in the template sequence represents TT, *cis-syn* T[]T or *cis-syn* T[]mC$^{m}$. **(B)** Primer extension assays using KF and hPolη. The primer-templates containing the *cis-syn* T[]T (lanes 2–8) and *cis-syn* T[]mC$^{m}$ (lanes 9–15) were incubated at 37°C with increasing amounts of KF (0.0125, 0.025, 0.1 units) or hPolη (8, 32, 128 fmol) for 15 min. The samples for lanes 3 and 9 contained no polymerases. For the positive control, the primer-template containing normal TT (lane 1) was also incubated with KF (0.1 units) at 37°C for 15 min. **(C)** Primer extension assays of the *cis-syn* T[]mC$^{m}$ (lanes 1–5) and *cis-syn* T[]T (lanes 6–10) in the presence of hPolη and each dNTP. The primer-templates were incubated with hPolη (8 fmol) at 37°C for 5 min. **(D)** Primer extension assays using dG17 (lanes 1–5) or T17 (lanes 6–10) primers in the presence of hPolη and each dNTP. The primer-templates were incubated with hPolη (16 fmol) at 37°C for 5 min.

**Table 2.** Kinetic parameters for nucleotide incorporation opposite the mC$^{m}$ moiety of T[]mC$^{m}$

| Substrates | $k_{cat}$ (min$^{-1}$) | $K_m$ (μM) | $k_{cat}/K_m$ (min$^{-1}$ μM$^{-1}$) | Efficiency |
|---|---|---|---|---|
| dGTP | 121 ± 12 | 18.7 ± 5.3 | 6.47 ± 1.94 | 1 |
| TTP | 172 ± 20 | 44.3 ± 11.2 | 3.88 ± 1.08 | 0.6 |

**Table 3.** Thermodynamic parameters for duplex formation

| Duplex | $\Delta H^{\circ}$ (kcal mol$^{-1}$) | $\Delta S^{\circ}$ (cal mol$^{-1}$ K$^{-1}$) | $\Delta G^{\circ}$ (kcal mol$^{-1}$)[a] | $T_m$ ($C_t$ = 12.0 μM) |
|---|---|---|---|---|
| TT·A | −84.5 ± 1.5 | −242 ± 4.4 | −12.3 ± 0.08 | 42.9 |
| TT·G | −63.8 ± 0.6 | −177 ± 1.6 | −11.0 ± 0.02 | 42.3 |
| TT·C | −54.9 ± 0.1 | −149 ± 0.3 | −10.5 ± 0.006 | 41.8 |
| TT·T | −52.1 ± 0.1 | −140 ± 0.2 | −10.3 ± 0.003 | 41.8 |
| T[]T·A | −80.4 ± 0.1 | −229 ± 0.4 | −12.0 ± 0.01 | 42.7 |
| T[]T·G | −56.8 ± 0.2 | −155 ± 0.6 | −10.7 ± 0.01 | 42.3 |
| T[]T·C | −48.6 ± 0.4 | −129 ± 1.1 | −10.0 ± 0.02 | 41.2 |
| T[]T·T | −53.3 ± 0.3 | −144 ± 0.9 | −10.3 ± 0.01 | 41.1 |
| TC·A | −79.4 ± 0.5 | −227 ± 1.5 | −11.8 ± 0.03 | 42.1 |
| TC·G | −93.3 ± 0.4 | −265 ± 1.1 | −14.2 ± 0.03 | 48.0 |
| TC·C | −68.9 ± 1.0 | −194 ± 2.8 | −11.1 ± 0.04 | 41.0 |
| TC·T | −66.6 ± 0.6 | −187 ± 1.7 | −10.9 ± 0.03 | 40.7 |
| TmC$^{m}$·A | −59.5 ± 0.02 | −164 ± 0.06 | −10.4 ± 0.001 | 40.2 |
| TmC$^{m}$·G | −74.2 ± 0.7 | −211 ± 2.1 | −11.4 ± 0.04 | 41.3 |
| TmC$^{m}$·C | −59.1 ± 0.3 | −163 ± 0.8 | −10.5 ± 0.01 | 40.8 |
| TmC$^{m}$·T | −58.5 ± 0.3 | −161 ± 0.8 | −10.5 ± 0.01 | 40.9 |
| T[]mC$^{m}$·A | −65.7 ± 0.8 | −183 ± 2.3 | −11.0 ± 0.04 | 41.4 |
| T[]mC$^{m}$·G | −92.1 ± 0.8 | −267 ± 2.3 | −12.6 ± 0.04 | 42.3 |
| T[]mC$^{m}$·C | −68.0 ± 0.5 | −191 ± 1.4 | −11.1 ± 0.03 | 41.6 |
| T[]mC$^{m}$·T | −85.0 ± 0.2 | −245 ± 0.7 | −12.1 ± 0.01 | 41.7 |

[a]At 25°C.

discuss the mechanism of nucleotide incorporation by hPolη.

Among the TT·N duplexes, TT·A was the most stable as expected, and its $\Delta G^{\circ}$ was −12.3 kcal mol$^{-1}$ (Figure 4A; Table 3). Upon CPD formation, the $\Delta G^{\circ}$ for T[]T·A was slightly increased by ∼0.3 kcal mol$^{-1}$, but the 3′ component of T[]T can form a stable base pair with adenine. The TC-containing 12-mer formed a stable duplex with the dG-ended 9-mer, and its $\Delta G^{\circ}$ was −14.2 kcal mol$^{-1}$, which is 2 kcal mol$^{-1}$ less, as compared with the other nucleobases. The most stable duplex among the TmC$^{m}$·N duplexes was the TmC$^{m}$·G, but its selectivity for G was much reduced compared to that of TC, probably because the *cis*-rotamer of mC$^{m}$ inhibited the formation of the Watson–Crick mC$^{m}$·G base pair (31,32). In the case of T[]mC$^{m}$, however, the stability of the mC$^{m}$·T pair was increased upon CPD formation, and its $\Delta G^{\circ}$ was −12.1 kcal mol$^{-1}$. The most stable duplex among the T[]mC$^{m}$·N duplexes was T[]mC$^{m}$·G, with a $\Delta G^{\circ}$ of −12.6 kcal mol$^{-1}$, and the reduced $\Delta G^{\circ}$ value compared to that for TmC$^{m}$·G suggested that the mC$^{m}$ moiety of the T[]mC$^{m}$ likely formed the Watson–Crick base pair with guanine (Figure 4B). These results suggested that the *N*-methyl group drastically changes the base-pairing ability of cytosine, and that the mC$^{m}$ moiety of T[]mC$^{m}$ can form a thermodynamically stable base pair with thymine, which causes the misincorporation of TMP opposite T[]mC$^{m}$ by hPolη.

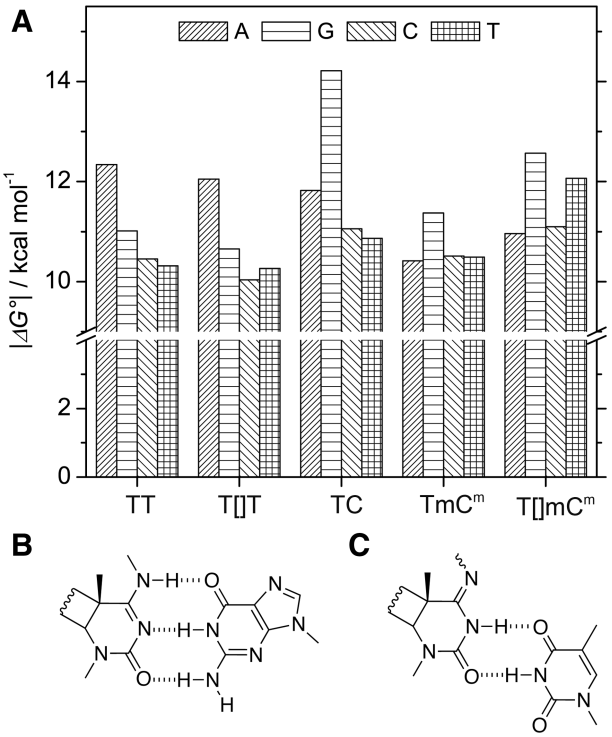


**Figure 4. (A)** Comparison of the thermodynamic stabilities of the base pairs at the 3′ component of CPD. Absolute values of Gibbs free energies (Table 3) are shown. **(B and C)** Plausible base pair formation by the $mC^m$ moiety of T[]$mC^m$ with guanine (B) and thymine (C).

## DISCUSSION

We synthesized partially protected thymidylyl-(3′→5′)-2′-deoxy-$N^4$,5-dimethylcytidine and performed its photosensitized [2 + 2] photocycloaddition, which resulted in the formation of the CPD between thymine and $N^4$,5-dimethylcytosine (T[]$mC^m$), without significant hydrolytic deamination. However, in this reaction, the *trans-syn* isomer, which is produced much less efficiently than the *cis-syn* CPD upon UV irradiation of isolated DNA (33), was the major product, in contrast to the low yield of the *cis-syn* isomer. Consistent with our previous report on the stereoselective CPD formation (18), the modification of the exocyclic amino group significantly affected the stereoselectivity of CPD formation, and the relative yield of the *cis-syn* isomer was lowered, due to the steric hindrance by the *N*-modification group. We also tested the photocycloaddition of thymidylyl-(3′→5′)-2′-deoxy-$N^4$-methylcytidine phosphotriester, which lacked the C5 methyl group within the $mC^m$ moiety of compound **4**. In this case, the *cis-syn* CPD (T[]$C^m$) was hardly detected, and the *trans-syn* isomer was produced predominantly, while the reaction using compound **4** gave the *cis-syn* T[]$mC^m$. This is the reason why we used mC. Notably, the *trans-syn* T[]$C^m$ was also stable enough to be purified as the intact form. This result indicated that the *N*-methyl modification of cytosine, rather than the C5 methyl group, was important for the resistance to hydrolysis.

To compare the thermal stabilities of T[]$mC^m$ and T[]mC, the $E_a$ and $A$ values for the hydrolysis of T[]mC were determined, using the kinetic parameters reported by Song *et al.* (17) (Table 1). It should be noted that a certain level of error may be included in the following values due to the differences in the experimental conditions, because several factors, such as ionic strength of the solution (34) and the nucleotides flanking the lesion (35), significantly influence the deamination rate. $E_a$ values in Table 1, apparently suggested that the *N*-methyl modification reduced the stability to hydrolysis. The hydrolytic deamination of cytosine is reportedly accelerated under acidic conditions (34), and the probability of the protonation of the N3 position of the $mC^m$ moiety would be increased, due to the electron-donating ability of the *N*-methyl group. This factor should have increased the sensitivity to temperature and reduced the activation energy. While the values of the activation energy were similar, the frequency factor was 650-fold smaller than that for T[]$mC^m$. This accounts for the strong resistance of T[]$mC^m$ to hydrolysis. The *N*-methylation of the exocyclic amino group directly reduces the hydrolysis frequency, due to its electron-donating ability. Vilkaitis and Klimasauskas reported a bisulfite sequencing method that displays $N^4$-methylcytosine, as well as mC (20). Although they did not discuss its mechanism, it can now be explained by the enhanced stability of the bisulfite-attached intermediate to hydrolysis, in a similar manner to the case of T[]$mC^m$.

T[]$mC^m$ blocked DNA synthesis by the replicative DNA polymerase, in the same manner as T[]T (Figure 3B). Since the stalled polymerases can be replaced with TLS polymerases in cells, the bypass of T[]$mC^m$ by Y-family DNA polymerases was investigated. In this study, we chose human DNA polymerase η as the TLS polymerase, to evaluate the effect on the *N*-methyl modification by comparing the results between this and previous (17) studies. Our biochemical analysis revealed that human DNA polymerase η preferentially incorporated dGMP opposite the $mC^m$ moiety of T[]$mC^m$, although TMP was also considerably incorporated. The efficiency of TMP incorporation opposite the $mC^m$ moiety was 60% of that of dGMP, and TMP incorporation strongly blocked further chain elongation. hPolη reportedly incorporated incorrect nucleotides opposite the cisplatin-induced intrastrand crosslinks between two guanines and *N*-2-acetylaminofluorene-modified guanine (AAF-G) (6). In the case of AAF-G, the kinetic analysis was performed. The efficiencies of incorrect nucleotide incorporation were 3–4% in total, and the incorporated incorrect nucleotides severely blocked the subsequent primer extension (25). As compared to these results, the misincorporation of TMP opposite T[]$mC^m$ occurred quite frequently. Yeast and human DNA polymerases η reportedly incorporated guanine opposite the mC moiety of T[]mC, and the misincorporation of adenine was observed at only one thirty-second of the frequency, as compared to the incorporation of guanine (17), suggesting that the *N*-methyl group would drastically change the base-pairing ability of the mC moiety.

The thermodynamic analysis of the duplexes mimicking the primer-template structure revealed that T[]$mC^m$

formed a stable base pair with thymine, and its stability was slightly lower than that of the T[]mC$^m$·G pair (Figure 4A). This result is in good agreement with our biochemical kinetic analysis of the incorporation efficiencies, and the misincorporation due to the mismatch formation can also be explained by the mechanistic study of hPolη in crystals (8). It is reported that an incoming nucleotide forms a base pair with the template nucleotide at a ground state prior to making the phosphodiester bond, and therefore once the incoming nucleotide and the other factors are accommodated properly in the active site, nucleotide incorporation can occur. The slightly less efficient incorporation of TMP than that of dGMP by hPolη would be caused by the different stabilities of the base pairs. The mC$^m$ moiety of T[]mC$^m$ can form a canonical Watson–Crick base pair with guanine, in which the methyl group protrudes into the major groove (Figure 4B). To discuss the T[]mC$^m$·T pair, a model structure showing the incorporation of TMP opposite the 3′ component of the T[]T, in which the incoming TMP was fitted to AMPNPP, was constructed by using the reported ternary complex structure (Supplementary Figure S9) (7). Since the O4 of the incoming TMP is located close to the N4 of AMPNPP, the O4 of TMP may be involved in hydrogen bond formation with the N4 of the mC$^m$ moiety of T[]mC$^m$. However, the N3 of the mC$^m$ moiety is too far away to form a hydrogen bond with the N3 of TMP. Since the $\Delta G^\circ$ of the T[]mC$^m$·T pair is comparable to that of the T[]mC$^m$·G pair (Figure 4A), it is unlikely that only one hydrogen bond is formed between the 3′ component of T[]mC$^m$ and TMP, in the geometry shown in Supplementary Figure S9. Taking into account the incorporation of TMP by hPolη, the CPD in the template strand should be rotated in the direction shown by the arrow, and the tautomerization of T[]mC$^m$ would enable the N3 and the O2 of the 3′ component of T[]mC$^m$ to form hydrogen bonds with the O4 and the N3 of TMP, respectively (Figure 4C). Since the 5′ and 3′ components of T[]mC$^m$ are bridged via the cyclobutane ring, the shifted position of the mC$^m$ moiety causes the incorrect positioning of the 5′ component of T[]mC$^m$, resulting in the blockage of further primer extension.

In conclusion, we performed the photocycloaddition reaction of thymidylyl-(3′→5′)-2′-deoxy-$N^4$,5-dimethylcytidine, and found that the obtained CPD, T[]mC$^m$, was quite stable to hydrolysis. Kinetic analyses indicated that the electron-donating *N*-methyl group reduces the frequency of T[]mC$^m$ hydrolysis. Biochemical analyses revealed that T[]mC$^m$ could be bypassed correctly by human DNA polymerase η, but the incorporation of the incorrect TMP caused a severe blockage of DNA synthesis. The *N*-methylation of cytosine is a simple modification, but unexpectedly modulated the chemical and biochemical properties of cytosine-containing CPDs. $N^4$-methylcytosine has been found in bacterial genomes as a minor base (19,36), but has not been detected in eukaryotes thus far, despite the development and improvement of analytical instruments and techniques. Since thermophilic bacteria also have putative Y-family DNA polymerases, such as the DinB and UmuC proteins (37), TLS by these proteins will be investigated in the future.

## SUPPLEMENTARY DATA

Supplementary Data are available at NAR Online.

## FUNDING

Management expenses grants from the Ministry of Education, Culture, Sports, Science and Technology, Japan. Funding for open access charge: Management expenses grants from the Ministry of Education, Culture, Sports, Science and Technology, Japan.

*Conflict of interest statement*. None declared.

## REFERENCES

1. Iwai,S. (2008) Pyrimidine dimers: UV-induced DNA damage. In: Herdewijn,P. (ed.), *Modified Nucleosides in Biochemistry, Biotechnology and Medicine*. WILEY-VCH Verlag GmbH & Co. KGaA, Weinheim, pp. 97–131.
2. Naegeli,H. and Sugasawa,K. (2011) The xeroderma pigmentosum pathway: decision tree analysis of DNA quality. *DNA Repair (Amst.)*, **10**, 673–683.
3. Burgers,P.M., Koonin,E.V., Bruford,E., Blanco,L., Burtis,K.C., Christman,M.F., Copeland,W.C., Friedberg,E.C., Hanaoka,F., Hinkle,D.C. *et al*. (2001) Eukaryotic DNA polymerases: proposal for a revised nomenclature. *J. Biol. Chem.*, **276**, 43487–43490.
4. Masutani,C., Kusumoto,R., Yamada,A., Dohmae,N., Yokoi,M., Yuasa,M., Araki,M., Iwai,S., Takio,K. and Hanaoka,F. (1999) The *XPV* (xeroderma pigmentosum variant) gene encodes human DNA polymerase η. *Nature*, **399**, 700–704.
5. Johnson,R.E., Prakash,S. and Prakash,L. (1999) Efficient bypass of a thymine-thymine dimer by yeast DNA polymerase, Polη. *Science*, **283**, 1001–1004.
6. Masutani,C., Kusumoto,R., Iwai,S. and Hanaoka,F. (2000) Mechanisms of accurate translesion synthesis by human DNA polymerase η. *EMBO J.*, **19**, 3100–3109.
7. Biertümpfel,C., Zhao,Y., Kondo,Y., Ramón-Maiques,S., Gregory,M., Lee,J.Y., Masutani,C., Lehmann,A.R., Hanaoka,F. and Yang,W. (2010) Structure and mechanism of human DNA polymerase η. *Nature*, **465**, 1044–1048.
8. Nakamura,T., Zhao,Y., Yamagata,Y., Hua,Y.-J. and Yang,W. (2012) Watching DNA polymerase η make a phosphodiester bond. *Nature*, **487**, 196–201.
9. Gonzalgo,M.L. and Jones,P.A. (1997) Mutagenic and epigenetic effects of DNA methylation. *Mutat. Res.*, **386**, 107–118.
10. Frederico,L.A., Kunkel,T.A. and Shaw,B.R. (1990) A sensitive genetic assay for the detection of cytosine deamination: determination of rate constants and the activation energy. *Biochemistry*, **29**, 2532–2537.
11. Barak,Y., Cohen-Fix,O. and Livneh,Z. (1995) Deamination of cytosine-containing pyrimidine photodimers in UV-irradiated DNA. *J. Biol. Chem.*, **270**, 24174–24179.
12. Horsfall,M.J., Borden,A. and Lawrence,C.W. (1997) Mutagenic properties of the T-C cyclobutane dimer. *J. Bacteriol.*, **179**, 2835–2839.
13. Takasawa,K., Masutani,C., Hanaoka,F. and Iwai,S. (2004) Chemical synthesis and translesion replication of a *cis-syn* cyclobutane thymine-uracil dimer. *Nucleic Acids Res.*, **32**, 1738–1745.
14. Douki,T. and Cadet,J. (1994) Formation of cyclobutane dimers and (6-4) photoproducts upon far-UV photolysis of 5-methylcytosine-containing dinucleotide monophosphates. *Biochemistry*, **33**, 11942–11950.
15. Celewicz,L., Mayer,M. and Shetlar,M.D. (2005) The photochemistry of thymidylyl-(3′-5′)-5-methyl-2′-deoxycytidine in aqueous solution. *Photochem. Photobiol.*, **81**, 404–418.
16. Vu,B., Cannistraro,V.J., Sun,L. and Taylor,J.-S. (2006) DNA synthesis past a 5-methylC-containing *cis-syn*-cyclobutane

pyrimidine dimer by yeast Pol η is highly nonmutagenic. *Biochemistry*, **45**, 9327–9335.
17. Song,Q., Sherrer,S.M., Suo,Z. and Taylor,J.-S. (2012) Preparation of site-specific T = mCG *cis-syn* cyclobutane dimer-containing template and its error-free bypass by yeast and human polymerase η. *J. Biol. Chem.*, **287**, 8021–8028.
18. Yamamoto,J., Nishiguchi,K., Manabe,K., Masutani,C., Hanaoka,F. and Iwai,S. (2011) Photosensitized [2 + 2] cycloaddition of *N*-acetylated cytosine affords stereoselective formation of cyclobutane pyrimidine dimer. *Nucleic Acids Res.*, **39**, 1165–1175.
19. Ehrlich,M., Wilson,G.G., Kuo,K.C. and Gehrke,C.W. (1987) $N^4$-methylcytosine as a minor base in bacterial DNA. *J. Bacteriol.*, **169**, 939–943.
20. Vilkaitis,G. and Klimasauskas,S. (1999) Bisulfite sequencing protocol displays both 5-methylcytosine and $N^4$-methylcytosine. *Anal. Biochem.*, **271**, 116–119.
21. Murata,T., Iwai,S. and Ohtsuka,E. (1990) Synthesis and characterization of a substrate for T4 endonuclease V containing a phosphorodithioate linkage at the thymine dimer site. *Nucleic Acids Res.*, **18**, 7279–7286.
22. Xu,Y.Z., Zheng,Q. and Swann,P.F. (1992) Synthesis of DNA containing modified bases by postsynthetic substitution. Synthesis of oligomers containing 4-substituted thymine: $O^4$-alkylthymine, 5-methylcytosine, $N^4$-(dimethylamino)-5-methylcytosine, and 4-thiothymine. *J. Org. Chem.*, **57**, 3839–3845.
23. Chaix,C., Molko,D. and Téoule,R. (1989) The use of labile base protecting groups in oligoribonucleotide synthesis. *Tetrahedron Lett.*, **30**, 71–74.
24. Creighton,S., Bloom,L.B. and Goodman,M.F. (1995) Gel fidelity assay measuring nucleotide misinsertion, exonucleolytic proofreading, and lesion bypass efficiencies. *Methods Enzymol.*, **262**, 232–256.
25. Kusumoto,R., Masutani,C., Iwai,S. and Hanaoka,F. (2002) Translesion synthesis by human DNA polymerase η across thymine glycol lesions. *Biochemistry*, **41**, 6090–6099.
26. Fujiwara,Y. and Iwai,S. (1997) Thermodynamic studies of the hybridization properties of photolesions in DNA. *Biochemistry*, **36**, 1544–1550.
27. Marky,L.A. and Breslauer,K.J. (1987) Calculating thermodynamic data for transitions of any molecularity from equilibrium melting curves. *Biopolymers*, **26**, 1601–1620.
28. Meyer,S.L. (1975) *Chapter 14: Straight-line Graphs and Fitting, Data Analysis for Scientists and Engineers*. John Wiley & Sons, New York, pp. 71–75.
29. Persmark,M. and Guengerich,F.P. (1994) Spectroscopic and thermodynamic characterization of the interaction of $N^7$-guanyl thioether derivatives of d (TGCTG*CAAG) with potential complements. *Biochemistry*, **33**, 8662–8672.
30. Taylor,J.S., Brockie,I.R. and O'Day,C.L. (1987) A building block for the sequence-specific introduction of *cis-syn* thymine dimers into oligonucleotides. Solid-phase synthesis of TpT[*c,s*]pTpT. *J. Am. Chem. Soc.*, **109**, 6735–6742.
31. Shoup,R.R., Miles,H.T. and Becker,E.D. (1972) Restricted rotation about the exocyclic carbon-nitrogen bond in cytosine derivatives. *J. Phys. Chem.*, **76**, 64–70.
32. Engel,J.D. and Hippel,P.H. (1974) Effects of methylation on the stability of nucleic acid conformations: studies at the monomer level. *Biochemistry*, **13**, 4143–4158.
33. Douki,T., Court,M., Sauvaigo,S., Odin,F. and Cadet,J. (2000) Formation of the main UV-induced thymine dimeric lesions within isolated and cellular DNA as measured by high performance liquid chromatography-tandem mass spectrometry. *J. Biol. Chem.*, **275**, 11678–11685.
34. Lemaire,D.G.E. and Ruzsicska,B.P. (1993) Kinetic analysis of the deamination reactions of cyclobutane dimers of thymidylyl-3′,5′-2′-deoxycytidine and 2′-deoxycytidylyl-3′,5′-thymidine. *Biochemistry*, **32**, 2525–2533.
35. Cannistraro,V.J. and Taylor,J.-S. (2009) Acceleration of 5-methylcytosine deamination in cyclobutane dimers by G and its implications for UV-induced C-to-T mutation hotspots. *J. Mol. Biol.*, **392**, 1145–1157.
36. Ehrlich,M., Gama-Sosa,M.A., Carreira,L.H., Ljungdahl,L.G., Kuo,K.C. and Gehrke,C.W. (1985) DNA methylation in thermophilic bacteria: $N^4$-methylcytosine, 5-methylcytosine, and $N^6$-methyladenine. *Nucleic Acids Res.*, **13**, 1399–1412.
37. Makarova,K.S., Aravind,L., Grishin,N.V., Rogozin,I.B. and Koonin,E.V. (2002) A DNA repair system specific for thermophilic Archaea and bacteria predicted by genomic context analysis. *Nucleic Acids Res.*, **30**, 482–496.